Mol Breeding (2023) 43:11
https://doi.org/10.1007/s11032-023-01355-7

Linkage and association mapping of ovule number per ovary (ON) in oilseed rape (*Brassica napus* L.)

Ali Ahmad · Wenhui Li · Hui Zhang · Hao Wang · Pengfei Wang · Yushun Jiao · Chenqi Zhao · Guangsheng Yang · Dengfeng Hong

Received: 11 October 2022 / Accepted: 11 January 2023 / Published online: 8 February 2023
© The Author(s), under exclusive licence to Springer Nature B.V. 2023

Abstract Ovule number (ON) produced during flower development determines the maximum number of seeds per silique and thereby affects crop productivity; however, the genetic basis of ON remains poorly understood in oilseed rape (*Brassica napus*). In this study, we genetically dissected the ON variations in a double haploid (DH) population and in natural population (NP) by linkage mapping and genome-wide association analysis. Phenotypic analysis showed that ON displayed normal distribution in both populations with the broad-sense heritability of 0.861 (DH population) and 0.930 (natural population). Linkage mapping identified 5 QTLs related to ON, including *qON-A03*, *qON-A07*, *qON-A07-2*, *qON-A10*, and *qON-C06*. Genome-wide association studies (GWAS) revealed 214, 48, and 40 significant single-nucleotide polymorphisms (SNPs) by individually using the single-locus model GLM and the multiple-locus model MrMLM and FASTMrMLM. The phenotypic variation explained (PVE) by these QTLs and SNPs ranged from 2.00–17.40% to 5.03–7.33%, respectively. Integration of the results from both strategies identified four consensus genomic regions associated with ON from the chromosomes A03, A07, and A10. Our results preliminarily resolved the genetic basis of ON and provides useful molecular markers for plant yield improvement in *B. napus*.

Keywords Ovule number · Genome-wide association study · Linkage mapping · QTLs · Double haploid · *Brassica napus*

Introduction

Oilseed rape (*Brassica napus* L., AACC) is mainly cultivated to produce edible oil from the seeds and ranks as the second-largest growing oil crop after soybean (Shi et al. 2015). As a complex quantitative trait, oilseed rape plant yield is systematically controlled by three major components, i.e., seed number per silique (SN), silique number per plant (SP), and seed weight (SW) (Wang et al. 2016). Among them, SN displays rich variations in both cultivars and germplasm resources, thus being an important breeding objective for rapeseed genetic improvement (Chen et al. 2011;

Supplementary Information The online version contains supplementary material available at https://doi.org/10.1007/s11032-023-01355-7.

A. Ahmad · W. Li · H. Zhang · H. Wang · P. Wang · Y. Jiao · C. Zhao · G. Yang · D. Hong (✉)
National Key Laboratory of Crop Genetic Improvement, Huazhong Agricultural University, Wuhan 430070, People's Republic of China
e-mail: dfhong@mail.hzau.edu.cn

G. Yang · D. Hong
Hubei Hongshan Laboratory, Huazhong Agricultural University, Wuhan 430070, People's Republic of China

Yang et al. 2017; Jiao et al. 2021). In flowering plants, ovules provide structural and ground support for the female gametophyte and develop into seeds after fertilization (Drews and Koltunow 2011; Shi and Yang 2011). Thus, the maximum SN is developmentally determined by ovule number per ovary (ON), while the final SN is also affected by the proportions of successful ovule fertilization and fertilized ovule development. Therefore, improvement in crop productivity requires understanding of the molecular pathways that control ovule initiation and development (Yuan and Kessler 2019).

In model plants like *Arabidopsis* and rice, the ovule initiation and developmental processes have been investigated, and more than 70 key genes have been revealed to be involved in ovule initiation and development (Qadir et al. 2021), including carpel meristem formation (CMM), ovule identity, primordia initiation, and integuments development (Skinner 2004; Shi and Yang 2011; Cucinotta et al. 2014). *AINTEGUMENTA* (*ANT*), *REVOLUTA* (*REV*), *CUP-SHAPED COTYLEDON* (*CUC1* and *CUC2*), and *SPATULA* (*SPT*) regulate the CMM formation (Ishida et al. 2000; Nole-Wilson et al. 2010; Nahar et al. 2012); *AGAMOUS* (*AG*), *SHATTERPROOF* (*SHP1*, *SHP2*) *SEEDSTICK* (*STK*), and *SEPALLATA* (*SEP*) control the ovule identity (Favaro et al. 2003; Pinyopich et al. 2003; Skinner 2004). *CUC1, CUC2 ANT and HUELLENOLS* regulate the ovule initiation and boundary establishment (Liu et al. 2000; Skinner 2004; Galbiati et al. 2013; Cucinotta et al. 2014). *HLL* and *ANT*, *AG,* and *BEL1* also play a role in the integument formation (Skinner et al. 2001; Azhakanandam et al. 2008). Hormonal signaling and interactions also play a vital role in the expression and regulation of these genes. Cytokinin-auxin interaction guides the ovule organogenesis via *PIN1* under the control of cytokinin response factors (Galbiati et al. 2013; Cucinotta et al. 2016). *CUC1* and *CUC2* regulate cytokinin homeostasis (Cucinotta et al. 2018), suggesting a complex gene network associated with hormone signaling involved in the ovule development process. Recently, two genes, *NEW ENHANCER of ROOT DWARFISM* (*NERD1*) and *OVULE NUMBER ASSOCIATED 2* (*ONA2*), were also identified to participate in the determination of ovule number during flower development (Yuan and Kessler 2019). However, compared to some other developmental processes or traits, the genetic factors determining ovule number remain largely elusive, especially in rapeseed..

To date, nearly hundred QTLs related to seed number (SN) were identified in rapeseed (Zhu et al. 2020; Raboanatahiry et al. 2022); among these, *qSS.C9* (*BnaC9.SMG7b*) is the only SN-related QTL cloned to date (Li et al. 2015). By contrast, the genetics of ON remains largely unexplored, and only few QTLs related to ON were revealed (Khan et al. 2019; Qadir et al. 2022) via GWAS. Recently the integration of linkage and association mapping has exhibited powerful capability in exploring potential genetic loci for economically important traits. He et al. (2017) identified a *RING*-domain gene (*BnaC03g63480D*) with a potential role in branch morphogenesis via GA modulation. Similarly, 12 growth period related genes, including *BnaTOC1.A03* and *BnaFUL.A03* were detected by integrating linkage and GWAS mapping (Wang et al. 2020b). The combination of association mapping and a linkage analysis can reduce false positives from associated loci due to high LD but also facilitates fine mapping of a target region with a large QTL interval (Hu et al. 2011); it can also narrow the target location to identify fewer candidate genes and reduce the timeline to gene cloning or identification of tightly linked markers for breeding.

Here, we analyzed the variations and genetic basis of ON both in a double haploid (DH) population based on linkage analysis and a panel of natural accessions by GWAS. Our work laid a foundation for map-based cloning of the genes responsible for the ON trait and will provide molecular markers for their improvement.

Materials and methods

Plant materials

A DH population comprised of 188 lines was used for the study, which was previously developed from the F_1 cross between two inbred accessions (ZY50 and 7–5) (Wang et al. 2020a). An association panel of 505 inbred lines collected from various geographic locations was previously described (Tang et al. 2021) and was utilized in this study. However, the phenotype data was collected for 374 inbred lines only in all four environments.

Field experiment

The DH lines and two parents were grown for three consecutive years (2015, 2016, and 2017) in the experimental farm of Huazhong Agricultural University, located at Ezhou, Hubei province, China (30.39° N, 114.88° E). The field was arranged in a randomized complete block design with 2 replications. Each line was grown in 2 rowed plots consisting of 24 plants. The length and width of the rows were 1.2 and 0.3 m, respectively. The ON data of the DH population was recorded from 2016 to 2018 in two environments and one in 2017. Therefore, five datasets were available for analysis designated as DH-EZ16-1, DH-EZ16-2, DH-EZ17, DH-EZ18-1, and DH-EZ18-2, respectively. The natural population was planted in two locations in the 2016–2017 growing season (Huazhong Agricultural University 30.59° N, 114.29° E and Modern Agricultural Science and Technology Innovation Demonstration Park of Sichuan Academy of Agricultural Sciences (30.65° N, 104.06° E). In 2017–2018, this population was planted in the experimental farm of Huazhong Agricultural University, located at Ezhou, Hubei province, China (30.39° N, 114.88° E). Each line was grown in two-rowed plots with 10–15 plants per row. The seeds were sown by hand, and the field management followed standard agricultural practice (Khan et al. 2020). ON data for the natural population were recorded in four environments designated as NP-WH17, NP-CD17, NP-WH18, and NP-EZ18.

Phenotyping, data collection, and analysis

To analyze the ovule number, freshly developed inflorescences (BBCH55-60) were collected from the main branches of selected plants. Three plants were randomly selected from each DH lines and inbreed accessions for sampling. These samples were fixed and stored in the formalin solution at room conditions. From each inflorescence, ten buds with close size (5–6 mm) were randomly selected and dissected, and the ovaries were excised carefully. The sampled ovaries were suspended in 90% alcohol solution for 24–48 h in 2-ml Eppendorf tubes and then washed with ddH_2O. After removing the water, the ovaries were dried in the tube and were suspended in chloral hydrate solution for 12 to 72 h for clearing. Subsequently, the ovaries were pressed between two glass slides to visualize the individual ovules and photographed under a SZX2-ILLT microscope (Olympus Corporation, Japan) mounted with an Olympus DP73 camera. The number of ovules for each ovary was manually counted. Descriptive statistical analysis of the phenotypic data was carried out using Microsoft Excel. The ANOVA and H^2 analysis were performed in R-software using *lmerMod* procedure (Bates et al. 2015).

Linkage, association mapping, and QTL analysis

The linkage map used in this study was previously described in Wang et al. (2020a). QTL analysis was performed by composite interval mapping (Zhao-Baang 1994) using WinQTL cartographer 2.5 software (http://statgen.ncsu.edu/qtlcart/WQTLCart.htm). The experiment-wise LOD threshold was determined by permutation analysis (Churchill and Doerge 1994) with 1000 permutations. LOD scores corresponding to $P = 0.05$ (3.1 for DH) were used for identifying significant QTL. The additive effect (A) and phenotypic variation explained (PVE) by individual QTLs were estimated. For designation and nomenclature of the detected QTLs, the recommendations of McCouch et al. (1997) were adopted. The QTL analysis was carried out on the phenotype of five datasets (DH-EZ16-1, DH-EZ16-2, DH-EZ17, DH-EZ18-1, and DH-EZ18-2). The QTLs were categorized as major and minor QTLs based on the PVE. QTLs with a PVE value of ~ 10 or ≥ 10 with LOD ≥ 3.1 were considered significant QTLs.

The information genomic variation map, population structure, and LD are available in Tang et al. (2021). The association analysis was carried out following single-locus GWAS (SL-GWAS), and multiple-locus GWAS (ML-GWAS) approaches simultaneously. TASSEL V5.0 software was used following generalized linear model (GLM) and mixed linear model (MLM) for the analysis. The GLM was subdivided into a naive model (only considering genotype and phenotype, genotype as an independent variable, phenotype as a dependent variable) and PCs model (adding the first five principal components as covariates to control population structure). MLM was divided into the K model (adding the relationship matrix as covariates) and the PCs + K model (adding the first five principal components and the relationship matrix as covariates). The number of valid tags and calculation threshold was evaluated by GEC software (Li et al. 2012).

Integration of QTL and GWAS results and candidate gene identification

The linkage and association mapping results were integrated according to He et al. (2017). The QTL intervals were aligned to the *Darmor-bzh* reference genome based on the physical location of the flanking markers for each QTL, and the corresponding QTL regions were extracted. The physical location of each association loci was mapped to the physical region of the QTL. The common regions identified by linkage and association mapping were further mined to identify the possible candidate genes. First, all the genes within 150 kb flanking region for each SNP loci were searched and extracted (He et al. 2017; Ikram et al. 2020). Next, the ZS11 homologues for each Darmor-bzh gene were identified from the BnPIR: *Brassica napus* pan-genome information resource (http://cbi.hzau.edu.cn/cgi-bin/bnapus/geneindex). The gene annotation and *Arabidopsis* homologue information were retrieved from BnTIR: *Brassica napus* transcriptome information resource (http://yanglab.hzau.edu.cn/BnTIR/expression_show). The expression of these genes was compared between ZY-50 and 7–5 (parental lines) at 3–4 mm, 4–5 mm, and 5–6 mm bud length. The genes showing extremely low expression or expressional difference less than two-fold between parental lines were not considered as candidate genes. Genes showing higher or more than two-fold expression differences between the parental lines were considered a putative candidate genes.

Results

Rich variations in ON were extensively observed in both the DH population and the natural inbred accessions

To investigate whether ON remained stable with the development of ovaries, we harvested the ovaries with consecutive sizes (2–7 mm) from the parental accessions. As shown in Fig. 1b, the results showed that the ovary size had no significant effects on the ON. Because large ovaries display obvious advantages in sample preparation and ON counting, 5–6 mm ovaries were used for observations in this study (Fig. 1a). The parental accession, ZY-50, had a smaller ON (25.85 ± 1.36) than 7–5 (32.92 ± 1.46) in all environments (Fig. 1c, Table S1), while ON of their derived DH lines ranged from 24.4 to 44.5, following the normal distribution with transgressive segregation (Figs. 2a and 3a and Table S1). ANOVA confirmed that the genotype of DH lines (G) and the growing environment (E) and genotype by environment ($G \times E$) interactions have significant effects on the ON phenotype. The broad-sense heritability of ON was 0.86 (Table S3). The ON phenotype data of the DH population showed a positive correlation across the environments (Fig. 3).

Similarly, we also found extensive variations for ON in the natural population across all the four environments, varying from 17.13 to 38.8 (Table S2). Normal distribution of ON was observed across the environments (Figs. 2b and 3b and Table S2), and the phenotypic correlation of ON was significantly positive among the four growing locations (Fig. 3). The ANOVA revealed that the genotype (G) and environment (E) had significant effects on the ON phenotype in the natural population (Table S4), and the broad-sense heritability of ON reached 0.93, indicating the stability of the ON and small effects of the environment on the trait.

Identification of QTLs linked with ON from the DH population

QTL mapping based on the DH population in five environments detected five loci for ON located on chromosomes A03, A07, A10, and C06, respectively (Fig. 4), with the detail information of each QTL given in Table 1. These QTLs explained 2.00–17.40% of the phenotypic variations for ON, respectively. *qONA-07–2* was detected in DH-EZ16-1, DH-EZ16-2, DH-EZ18-1, and DH-EZ18-2, and *qON-C06* was detected in three environments (DH-EZ16-2, DH-EZ18-1, and DH-EZ18-2). *qON-A07-1* was detected in DH-EZ16-1 and DH-EZ16-2, while *qON-A10* was detected in the DH-EZ16-1 and DH-EZ17 environments. *qON-A03* was observed only in the DH-EZ16-1 environment (Table 1). The linkage and physical locations of these QTLs are also visualized on Circos (Fig. 4).

From these QTL, we found that *qONA-07–2* and *qON-A10* show larger effects, with the PVE of 17.38% and 9.32%, respectively. The confidence intervals for these QTLs were individually 27 cM and

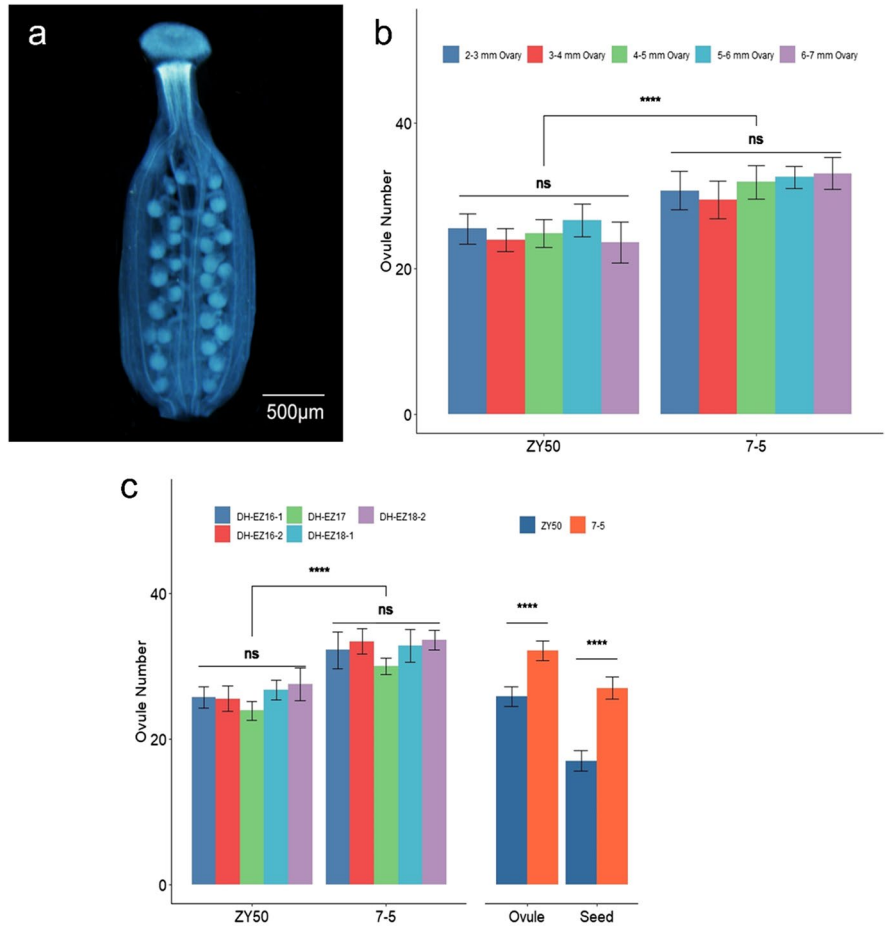

Fig. 1 Observation of the ON. **a** A 6-mm ovary excised from unopened floral bud with visualized ovules. **b** Comparison of ON in ovaries of various length ranging from 2 to 7 mm ZY50 and 7–5. **c** Comparison of ON between ZY-50 and 7–5 in different environments, average ON and SN of ZY50 and 7–5

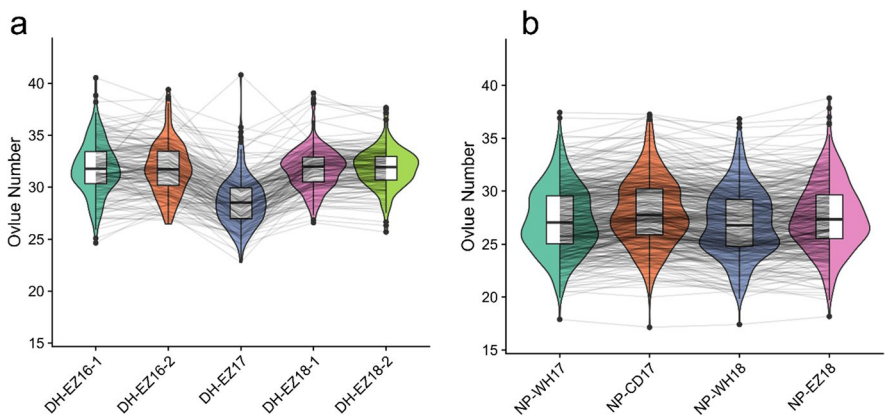

Fig. 2 Phenotypic variations and distribution of ON in the **a** DH and **b** natural population. Violins and box plots depict the phenotypic distribution of DH lines (5 environments) and natural population (4 environments)

26 cM for *qONA-07–2* and *qON-A10* on the linkage map. Correspondingly, the candidate physical interval of *qONA-07–2* is about 5.75 Mb on chromosome A07, while the *qON-A10* has a 3.65 Mb physical interval on chromosome A10.

Association mapping analysis

GWAS was carried out for four environment and BLUP using GLM model (Fig. 5, Fig. S1). The GLM method detected 247, 757, 148, 80, and

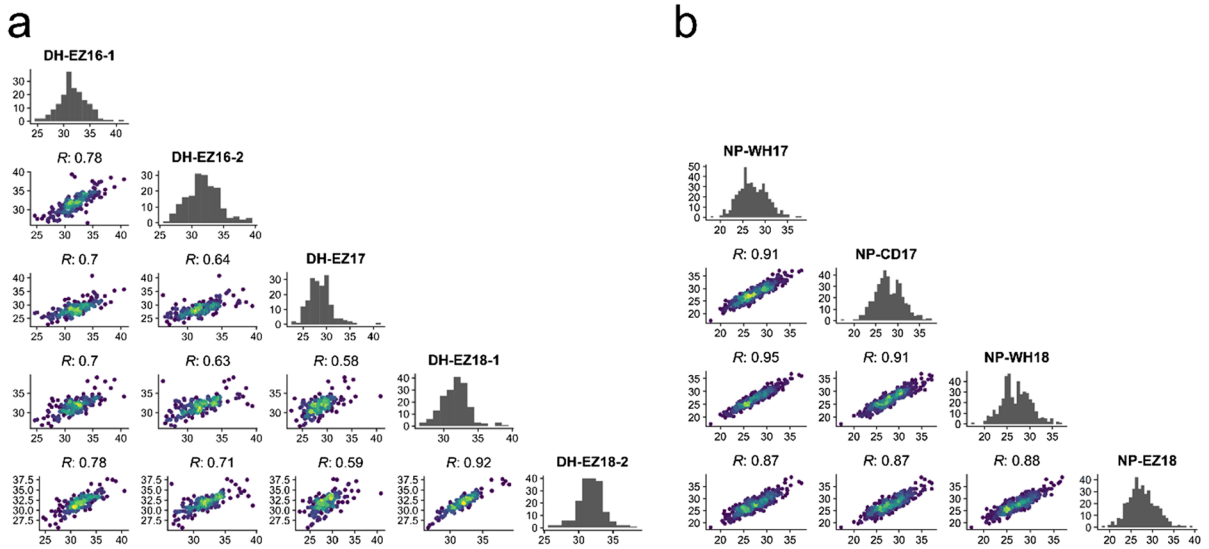

Fig. 3 Correlation of ON among different environments; **a** DH population and **b** natural population

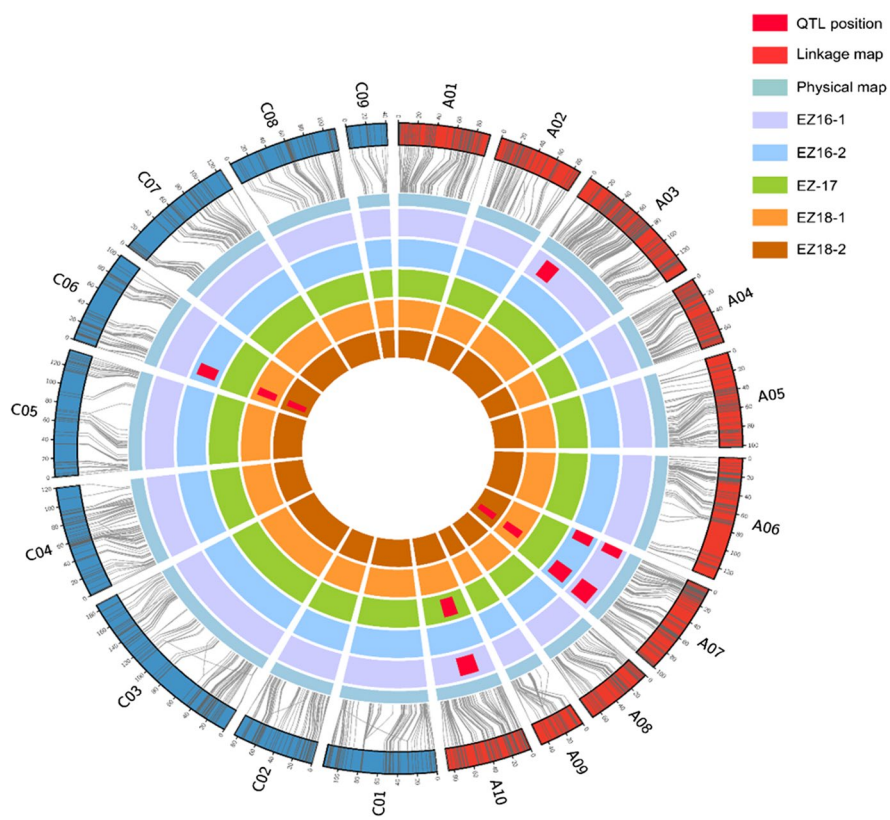

Fig. 4 Genetic linkage map of ON based on ZY50-75 DH population. Different environments are indicated by different color backgrounds on the cycle. From outside to inside, five cycles represent five environments, EZ16-1, EZ16-2, EZ17, EZ18-1, and EZ18-2, respectively. The two outer-most cycles represent comparison of linkage map and physical map of *B. napus*. Red bars within the cycles indicate QTL regions on chromosomes

Table 1 Summery of the detected QTLs for ON in the *ZY-50–7-5* DH population

QTL	Chromosome	Environment	CI (cM)	Peak	LOD	*A*	PVE (%)	Marker interval	Peak	Physical location (bp)
qON-A03	A03	DH-EZ16-1	17.13–39.08	28.88	4.62	−0.71	6.26	SNP7246–SNP7842	SNP7577	2,489,789–6,449,394
qON-A07-1	A07	DH-EZ16-1	0.00–14.30	5.30	5.18	−0.86	9.00	SNP16055–SNP17293	SNP22237	288,096–8,992,489
qON-A07-1	A07	DH-EZ16-2	0.00–18.00	6.89	2.74	0.40	15.50			
qON-A07-2	A07	DH-EZ16-1	67.07–94.54	71.70	6.69	−0.91	10.15	SNP15827–SNP16479	SNP16241	17,276,283–23,034,737
qON-A07-2	A07	DH-EZ16-2	66.12–92.54	80.46	5.72	−0.92	17.38			
qON-A07-2	A07	DH-EZ18-1	57.65–77.71	71.70	5.78	−0.65	11.12			
qON-A07-2	A07	DH-EZ18-2	57.65–77.71	71.70	7.79	−0.70	14.47			
qON-A10	A10	DH-EZ16-1	22.27–48.97	37.67	6.62	0.88	9.28	SNP23717–SNP22394	SNP21963	9,684,802–13,259,784
qON-A10	A10	DH-EZ17	22.27–48.97	37.14	6.69	0.75	9.32			
qON-C06	C06	DH-EZ16-2	10.5–31.13	23.93	4.85	−0.81	1.90	SNP45475–SNP26603	SNP41089	5,403,297–15,952,791
qON-C06	C06	DH-EZ18-1	15.01–33.86	21.93	3.83	−0.53	7.40			
qON-C06	C06	DH-EZ18-2	15.01–33.86	26.75	2.96	−0.41	4.85			

CI confidence interval, *A* additive effects, *PVE (%)* percentage of variations explained

214 significant QTNs in NP-WH17, NP-CD17, NP-WH18, NP-EZ18, and BLUP, respectively. The significant QTNs in NP-WH17 were detected on chromosomes A02, A07, A08, A10, C02, C03, C06, and C08. The QTNs detected in NP-CD17 were located on chromosomes A02, A03, A06, A08, A09, A10, C02, C03, C06, and C08. In NPWH18, the significant QTNs were located on chromosomes A01, A02, A07, A08, A09, C02, C03, and C04, while in NP-EZ18, the significant QTNs found on chromosomes A02, A06, A07, A08, C02, C08, and C09. The significant QTNs in BLUP were located on chromosomes A02, A07, A08, A09, C02, C03, C04, C06, and C08 (Fig. S1, Supp File S1). The PVE by these QTNs ranged between 5.03 and 7.33%, suggesting that ON is controlled by multiple genes with a small effect in the association panel.

Further, we performed ML-GWAS approaches, including MrMLM and FAST-MrMLM, on the same datasets as individual environments and the BLUP. Using mrMLM, we detected 46 QTNs in NP-WH17 and NP-CD17 each, 41 in NP-WH18, 37 in NP-EZ18, and 48 in BLUP. The PVE of these QTNs ranged between 3.92 and 21.22%. The FAST-MrMLM identified 44 QTNs in NP-WH17, 47 in NP-CD17 CD, and 46 in NP-WH18, while 40 SNPs in NP-EZ18 and 40 QTNs in BLUP (Fig. S2, Supp File S1). The explained PVE of these SNPs ranged from 3.73 to 21.20%.

Comparison of the QTLs between DH and association mapping

The physical location of each QTL from the DH population and SNP loci from the natural population was compared to mine the common loci between the two populations. The linkage analysis detected QTLs on chromosomes A03, A07, A10, and C06, while the association analysis identified loci on chromosomes A02, A03, A07, A08, A10, C02, C03, and C06 for ON. By integrating linkage and association mapping loci, four common genomic regions were identified on chromosomes A03, A07 and A10. Within these genomic regions, 31 significant SNPs were distributed (Table 2). Eight significant SNPs on chromosome A03 detected in GWAS were located in the CI of *qON-A03* (2.48–6.44 Mb). Five SNPs detected by GWAS fall within the CI of *qON-A07-1* (0.28–8.99 Mb). Twelve significant SNPs were detected in the CI of *qON-07–2*

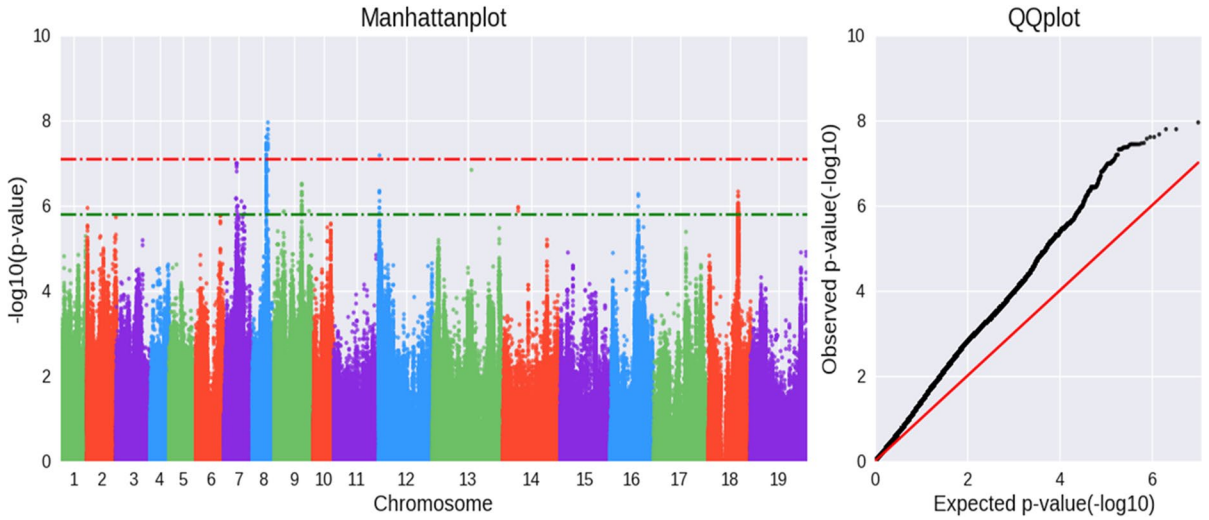

Fig. 5 Manhattan and QQ plot in the detection of SNPs for ON using single-locus GWAS based on BLUP values (green dashed line, suggestive threshold; red dashed, significant threshold)

physical region. In *qON-A07-2*, five SNPs are clustered within 400-bp interval (17,249,274 ~ 17,249,692). Six SNPs on chromosome A10 detected in GWAS overlapped with the CI of *qON-A10* (9.6–13.25). Among these six SNPs, three are clustered in a ~ 240 bp region (11,839,872 ~ 11,840,110). Furthermore, C06 also harbored three loci detected in GWAS and one QTL, *qON-C06*; however, the physical locations of these loci and QTLs were separated by large genomic interval (23.95 Mb and 5–15 Mb, respectively).

Candidate gene prediction

We then analyzed the annotated genes in the consensus regions identified commonly by linkage mapping and GWAS. A total of 269 genes distributed in the flanking regions of 12 significant SNPs located in *qON-A07-2*, while 145 genes flanked around the 6 SNPs located in *qONA-10*. According to the expression data derived from the developing flower buds of ZY-50 and 7–5, we further selected 54 and 37 putative genes from the candidate regions of *qON-A07-2* and *qON-A10*, respectively (Fig. 6, Supp File 2).

Based on the functional annotations of the putative candidate genes located in the *qON-A07-2* interval, we speculated that several genes might be involved in ON determination, including *BnaA07g22900D*, *BnaA07g27510D*, *BnaA07g25810D*, *BnaA07g27570D*, and *BnaA07g27740D*. *BnaA07g22900D* is an orthologue of *Arabidopsis* gene *HTH* (*AT1G72970*), which has been reported to be involved in floral organ development. The mutants showed an aberrant embryo sac development, floral organ fusion, and defective ovules (Lolle et al. 1998; Krolikowski et al. 2003; Pagnussat et al. 2005). The *Arabidopsis CML23* (*AT1G66400*) is orthologue to *BnaA07g25810D*. *CML23* reported to be involved in plant development and transition to reproductive phase. *CML23* in conjugation with *CML24* regulated floral organ development (Tsai et al. 2007; Nie et al. 2017; He et al. 2020). *BnaA07g27510D* is an orthologue of *Arabidopsis* gene *SOFL* (*AT1G68870*). *SOFL1* and *SOFL2* are positive regulator of cytokinin homeostasis and CK-mediated development (Zhang et al. 2006, 2009). *CIB1* (*AT1G68920*) is the *Arabidopsis* orthologue for *BnaA07g27570D*. *CIB1* is basic-helix-loop-helix (bHLH) transcription factor that regulate floral initiation (Liu et al. 2013). *BnaA07g27740D* is the orthologue of the *Arabidopsis CRC* (*AT1G69180*). Previous studies report *CRC* to be an ovule development and floral organ development regulator (Kuusk et al. 2002; Orashakova et al. 2009; Skinner and Gasser 2009; Liao et al. 2020). Knockdown of CRC orthologue in *E. californica* and *P. sativum* caused defective carpel and ovule initiation (Orashakova et al. 2009; Fourquin et al. 2014). *BnaA07g31240D* is orthologue to *Arabidopsis EXT3/RSH* (*AT1G21310*). *EXTINSINs* reportedly functions in call wall assembly in the rapidly growing cell in meristems (Saha et al. 2013; Choudhary et al. 2015). We also found some genes that showed high expressional abundances

Table 2 Consensus loci between DH and natural population for ON

Chromosome	QTL	Physical location of the QTL	Physical location SNP (QTN)	PVE % (QTL-GWAS locus)	Method	Environment	Remarks
A03	qON-A03	2,489,789–6,449,394	2,975,797	6.26, 4.58	2	WH2	Overlapping
			4,337,109	6.26, 5.96	2	WH2	Overlapping
			4,235,973	6.26, 8.69	2, 3	WH1, CD, EZ	Overlapping
			4,871,308	6.26, 9.28	2	WH1, B	Overlapping
			4,871,264	6.26, 5.08	2	WH1	Overlapping
			5,089,499	6.26, 7.30	2	CD	Overlapping
			6,526,587	6.26, 7.84	3	B	Overlapping
			5,175,003	6.26, 4.00	3	WH2	Overlapping
A07	qON-A07-1	288,096–8,992,490	5,066,540	9.00–15.50, 4.46	2	EZ	Overlapping
			623,642	9.00–15.50, 7.17	3	EZ	Overlapping
			882,064	9.00–15.50, 8.74	2	WH2	Overlapping
			2,332,818	9.00–15.50, 8.30	2	WH1	Overlapping
			7,476,139	9.00–15.50, 11.39	2, 3	WH1, WH2, B	Overlapping
	qON-A07-2	17,276,283–23,034,737	17,294,274	10.15–17.38, 9.97	1	CD	Overlapping
			17,294,318	10.15–17.38, 6.27	1	CD,	Overlapping
			17,294,456	10.15–17.38, 5.15	1	CD, B	Overlapping
			17,294,645	10.15–17.38, 5.15	1	CD, B	Overlapping
			17,294,692	10.15–17.38, 5.15	1	CD, B	Overlapping
			17,357,369	10.15–17.38, 5.13	3	EZ	Overlapping
			19,009,010	10.15–17.38, 4.29	3	CD, B	Overlapping
			20,003,845	10.15–17.38, 11.22	3	WH2	Overlapping
			20,113,568	10.15–17.38, 4.87	2	B	Overlapping
			21,878,438	10.15–17.38, 7.18	2	CD	Overlapping
			21,966,878	10.15–17.38, 6.2	2	WH1	Overlapping
			22,292,821	10.15–17.38, 5.76	3	WH2	Overlapping
A10	qON-A10	9,684,802–13,259,784	11,705,557	9.28–9.32, 6.26	2	CD,	Overlapping
			11,839,872	9.28–9.32, 0.05	1	CD	Overlapping
			11,840,073	9.28–9.32, 0.05	1	CD	Overlapping
			11,840,110	9.28–9.32, 0.05	1	CD	Overlapping
			12,594,051	9.28–9.32, 11.54	3	WH1	Overlapping
			12,828,274	9.28–9.32, 5.06	3	WH2	Overlapping

Methods (GLM, 1; MrMLM, 2; FASTMrMLM, 3), environments, (NP-WH17, WH1; NP-CD17, CD; NP-WH18, WH2; and NP-EZ18, EZ; BLUP, B)

at the bud level but uncharacterized functions, including BnaA07g27560D (*AT1G68910*), *BnaA07g27670D* (*AT1G69050*), and *BnaA07g27750D* (*AT1G69200*).

Similarly, we also identified several genes with known functions that could be related to ON formation from the candidate region of *qON-A10*. *BnaA10g14760D* is an orthologue of *AT5G20730* that encodes auxin response factor (*ARF7*). The *ARF7* create auxin responsiveness in *MND1* and regulate plant development (Li et al. 2021).. *BnaA10g14910D* is the orthologue of *Arabidopsis AT5G20570* that encodes *RING-BOX / RBx1*. *AtRBx1* is part of the SCF-complex an E3-Ubiquitine ligase. Downregulation of *AtRBx1* impair developmental aspects including floral development (Ni et al. 2004; Bernhardt et al. 2006; Chen et al. 2006). *AT5G17300 is the Arabidopsis* orthologue of *BnaA10g17370D* that encodes *REVEILLE* (*RVE1*). *RVE1* is Myb-like transcription factor that regulate the auxin level. *RVE1* is reported to be expressed in ovule primordia (Skinner and Gasser 2009), hypocotyl growth, auxin response, and seed

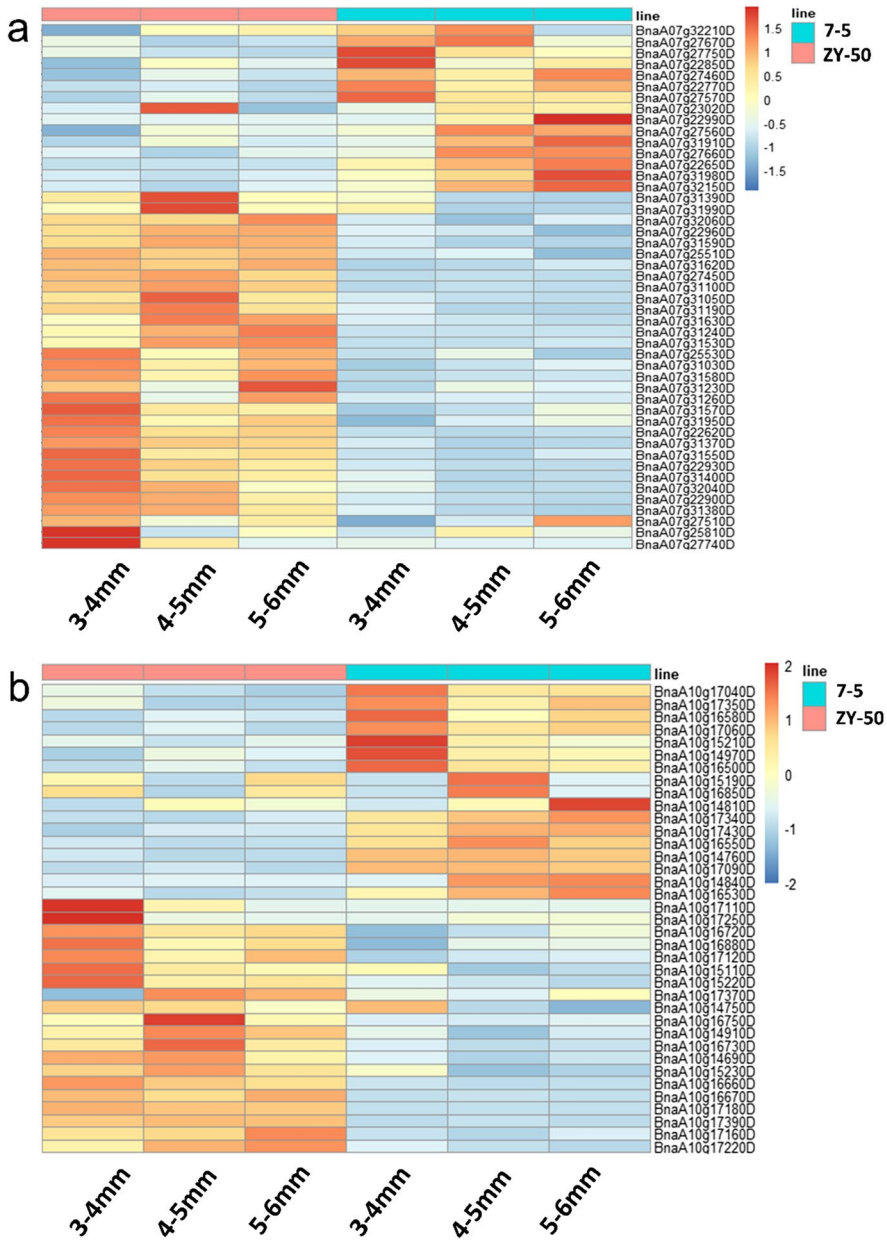

Fig. 6 Differential expression of genes predicted in qON-07–2 and qON-A10 regions (FPKM)

development (Rawat et al. 2009; Jiang et al. 2016). *BnaA1017060D* is orthologue of *AT5G17690* that encodes *LHP1*. *LHP1* cooperate with *BP*C and *MADS*-domain factors to orchestrates the *SKT* activity during floral development (Petrella et al. 2020). *BnaA10g16730D* is orthologue to *AT5G18090* that encodes an *AP2/B3* like transcription factor that belongs to *REM* family. The *REM* family genes are involved in early stage of floral and ovule primordia development (Kelley and Gasser 2009; Mantegazza et al. 2014). In wheat *AP2-like* transcription factors (*AP2L2* and *AP2L5*) are redundantly involved in floral development and regulate MAD-Box floral genes (Debernardi et al. 2020). In the *qON-A10* interval, some genes showed high expressional abundances at the bud level but uncharacterized functions, including *BnaA10g16530D (AT5G18310)*, *BnaA10g17120D (AT5G17620)*, *BnaA10g17220D (AT5G17510)*, *BnaA10g17250D (AT3G03341)*, and *BnaA10g17390D (AT5G17280)*.

Integration of the known QTLs for SY-related traits

To assess whether the QTLs detected in the present study are in the genomic regions important for oilseed rape breeding, we compared the physical interval of our QTLs with the previously reported QTLs. The comparison was restricted to SY-related traits only, like seed number (SN), the number of silique/pods (NP), and seed weight (SW) in different mapping populations following Raboanatahiry et al. (Raboanatahiry et al. 2018, 2022). We searched the previously published QTLs within the physical interval of the QTLs detected in our study (Table 1). Several loci related to SN, SW, NP, SL, biomass, and SY were found within the interval of our QTLs (Supp File S3). Interestingly, all the overlapping loci were found to be located on the A genome.

In total, 118 previously reported loci were identified that overlap with four QTL identified in our study. Further observation revealed that majority of these loci is related to SW and SN. It is crucial to identify regions that influence multiple traits, especially the closely related traits, i.e., SW and SN. The *qON-A03* CI includes 18 previously reported loci. These loci are related to SW (7), NP (2), and SY (9 loci) (File S3). Forty-three previously reported loci were found in the *qON-A07-1* interval. Among these, five loci are related to SN, twenty-seven related to SW, three related to biomass, and four loci are SY related. The *qON-A07-2* interval harbors thirty-four loci. Among these, fourteen loci are related to SN, and two (SW), five (biomass), eight (SP), and four are SY-related loci. Within the *qON-A10* interval, 23 previously reported SY-related overlaps (File S3). The *qON-A07-1* interval was found to have the highest number of overlapping regions (34) with previous studies. In combination with the previous studies and present results, it can be concluded that these genomic regions might be of great potential for oilseed rape breeding.

Discussion

QTL mapping has been proved to be a potential tool to unveil the genetic mechanisms of complex agronomic traits (Wang et al. 2020a) and is frequently utilized in *B. napus* for several traits. The combination of linkage and association mapping approaches further aids the detection by identifying common and stable loci with strong genetic control of the trait (Hu et al. 2011; He et al. 2017). In the present study, we investigated the phenotypes and genetics of ON through a biparental population and in a natural population consisting of comprehensive inbred accessions in different environments. We found that ON showed a wide range of variations in both populations inheriting as a typical quantitative trait. The ON data was subjected to linkage and association analysis. This study identified five ON-related QTLs via linkage mapping while 214 significant loci via association mapping (SL-GWAS). MrMLM and FASTMrMLM (ML-GWAS) also detected 48 and 40 significant loci associated with ON. Interestingly, both approaches identified common genomic regions that control the ON. This ascertains the accuracy of our mapping results as both approaches augment each other. To further intuit the accuracy of the identified loci, the genomic regions underlying these loci were compared to the previously reported SY-related QTLs. Since previous studies associated with yield-related traits in oilseed rape majorly focused on SN, SP, SL, and SW, our findings will strengthen understanding of the genetic basis of yield components in oilseed rape.

The strategy of combining linkage mapping with association mapping has been proposed to promote the identification of the causal genes for a quantitative trait (He et al. 2017; Wang et al. 2020a). Linkage mapping utilizes and associates recent recombination events (biparental populations) to the traits, while association mapping relies on the historic recombination (natural populations) accumulated over the course of time (Nordborg and Weigel 2008; Li et al. 2014). Therefore, the combination of both approaches might be helpful in uncovering the consensus loci based on recent mutations or recombination. In the present study, consensus loci were found on ChrA03, A07, and A10 in linkage mapping and GWAS (Table 2). Four QTLs on the A genome (*qON-A03*, *qON-A07-1*, *qONA-07–2 qON-A10*) overlapped with the SNPs detected in the association analysis. Among these consensus genomic regions, the major effect QTLs (*qON-A07-2* and *qON-A10*) were searched for the putative candidate genes. These results suggest that common loci detected in linkage and association are stable loci and provide strong genetic control of the traits (He et al. 2017). Linkage and association approaches have been used simultaneously to identify

QTLs in oilseed rape and cotton (He et al. 2017; Liu et al. 2018) to detect branch morphogenesis and fiber quality-related loci. However, the possibility of consensus loci identification is low because of the genetic backgrounds of biparental and natural populations. The consensus genomic regions identified in our study carry important genes involved in the floral and morphological development, cell fate, and specification and hormonal response, particularly auxins and cytokinin. The role of auxins and cytokinin and their crosstalk in ovule initiation and development is well elucidated in *Arabidopsis* (Galbiati et al. 2013; Cucinotta et al. 2016). Functional analysis of these genes in oilseed rape will open up new ways towards understanding the molecular mechanism of ovule development and number determination.

In *B napus*, 2,438 QTLs have been identified for 79 yield-related traits (Raboanatahiry et al. 2022). Several of these identified QTLs overlap or coincide with each other. Further, these QTLs were also found to affect other traits (Raboanatahiry et al. 2022). QTL comparison or colocalization from different mapping population having diverse genetic backgrounds aids the identification and validating stable loci (Li et al. 2018). Several QTLs reported in the previous were found to overlap or correspond to the QTLs identified in this study. However, we only selected the direct yield component traits for comparison to our QTLs. For instance, the *qONA*-3 likely corresponds to SW QTLs; *qSW.A03-1*, *qSW012*, and *DHqSW06* (Shi et al. 2009, 2011; Wang et al. 2020a). We identified and co-located 118 previously reported loci to our present QTLs. Among these 27 QTLs for SW, 22 for SN, 12 for SP, and 12 were collated for SY. The *qONA-3* and *qSW.A03-1* were detected in the same DH population. Similarly, the *qON-A07-1* and *qON-A07-2* are likely to complement to *TSWA7a*, cqSW.A07-1, *TSWA7b*, and c*qSW.A07-2*, (Fan et al. 2010; Wang et al. 2020a). The overlapping loci that affect multiple traits might be suitable for selection to improve the desired traits, simultaneously (Raboanatahiry et al. 2022). In *B. napus*, several QTLs have been reported that could influence more than one trait simultaneously (Jiao et al. 2021; Raboanatahiry et al. 2022; Liu et al. 2022). Integrating QTLs with overlapping intervals for different traits obtained significant co-localization of QTLs or pleiotropic QTLs (Zhao et al. 2016, 2019). This colocalization of QTLs from different traits indicates a strong inter-relationship or dependence on each other (Wang et al. 2010; Xin et al. 2021). This also suggests that these loci contain many tightly linked trait-specific genes or genes that affect multiple traits (Hall et al. 2006). This further suggests that the selection of these loci might aid the simultaneous improvement in more important traits. The *qON-A07-2* and *qON-A10* control ON, however its overlapping QTLs in other populations the control SN, SW and SP. Selection of these loci in breeding program will be helpful for simultaneous imprudent in other yield component traits, i.e., SN.

In recent GWAS studies, Khan et al. (2019) and Qadir et al. (2022) analyzed SN, SW, and ON and reported 8 and 18 significant SNPs associated with ON. However, comparing these results, no common QTN was found for ON. By contrast, Khan et al. (2019) identified five SW and five SN-related SNPs that overlap in the QTL intervals *qON-A03* (3), *qON-A07-1* (1), *qNO-A07-2* (1), and *qON-A10* (5). Interestingly, one of these SNP on chromosome A03 corresponds to *BnaA03g55500D* (GA20OX3: Gibberellin 20-oxidase 3). Two SNPs on the A10 corresponds to *BnaA10g12800D* (*GASA10*: Gibberellin-regulated family protein) and *BnaA10g16730D*, respectively. *BnaA10g16730D* is a homologue of the *Arabidopsis* gene *AT5G18090* that encodes an AP2/B3-like transcriptional factor family protein. Since *AP2* was previously reported to regulate the floral organ patterning, including ovule and ON number in *Arabidopsis* (Modrusan et al. 1994; Elliott et al. 1996; Krizek 2009; Huang et al. 2013), it is likely to speculate that *BnaA10g16730D* is a candidate of *qON-A10*. At unopened bud level, ZY-50 and 7–5 shows 5–tenfold expression differences (Fig. 6, Supp File S2). The expression differences between ZY-50 and 7–5 for *BnaA10g16730D* possibly suggest its involvement in ON development. However, the functional validation of these genes in oilseed rape is important to confirm the possible role and elucidate the understanding of ON development and number control.

Conclusion

We performed linkage mapping and association analysis based on a DH population and a panel of inbred accessions, respectively, to preliminarily determine the genetic structure of ON. The results

showed that ON could inherit with a high broad inheritability. Linkage and association mapping co-detected consensus in four genomic regions on chromosomes A03, A07 and A10. These loci contain 8, 5, 12, and 6 SNPs. Two QTL, *qON-A07-2* and *qON-A10*, show a relatively major effect. Based on the results from the linkage and association mapping, it can be concluded that several loci control the ON with small effects on the phenotype. Conceivably, these common loci may be conserved among the genetically diverse population causing variations in the phenotype. The putative genes underlying these loci are related to floral development, hormonal signaling, and carbohydrate metabolism. Understanding the role of these loci in the ovule development and determination will contribute to the yield potential of oilseed rape.

Author contribution AA, WL, DH, and GY designed and conceived and AA, WL, HZ, HW, PW, and JY performed the experiment. AA and DH wrote and drafted the manuscript. DH revised the manuscript. All authors contributed to the article and approved the submitted version.

Funding This research was supported by the National Key R&D Program of China (2022YFD1200400), Natural Science Foundation of Hubei Province (2019CFA090) and the National Natural Science Foundation of China (32072099 and 31971977).

Data availability The datasets supporting the results of this article are included within the article and its additional files. The DH population linkage mapping information is available in Wang et al. (2020a). The association mapping population data can be found in the Genome Sequence Archive (https://bigd.big.ac.cn/gsa/) with Bioproject IDs PRJCA002835 and PRJCA002836 (Tang et al. 2021).

Declarations

Ethics approval and consent to participate Not applicable.

Consent for publication Not applicable.

Competing interests The authors declare no competing interests.

References

Azhakanandam S, Nole-Wilson S, Bao F, Franks RG (2008) SEUSS and AINTEGUMENTA mediate patterning and ovule initiation during gynoecium medial domain development. Plant Physiol 146:1165–1181. https://doi.org/10.1104/pp.107.114751

Bates D, Mächler M, Bolker BM, Walker SC (2015) Fitting linear mixed-effects models using lme4. J Stat Softw 67:1. https://doi.org/10.18637/jss.v067.i01

Bernhardt A, Lechner E, Hano P et al (2006) CUL4 associates with DDB1 and DET1 and its downregulation affects diverse aspects of development in Arabidopsis thaliana. Plant J 47:591–603. https://doi.org/10.1111/j.1365-313X.2006.02810.x

Chen H, Shen Y, Tang X et al (2006) Arabidopsis CULLIN4 forms an E3 ubiquitin ligase with RBX1 and the CDD complex in mediating light control of development. Plant Cell 18:1991–2004. https://doi.org/10.1105/tpc.106.043224

Chen W, Zhang Y, Yao J et al (2011) Quantitative trait loci mapping for two seed yield component traits in an oilseed rape (Brassica napus) cross. Plant Breed 130:640–646. https://doi.org/10.1111/j.1439-0523.2011.01886.x

Choudhary P, Saha P, Ray T et al (2015) EXTENSIN18 is required for full male fertility as well as normal vegetative growth in Arabidopsis. Front Plant Sci 6:1–14. https://doi.org/10.3389/fpls.2015.00553

Churchill GA, Doerge RW (1994) Empirical threshold values for quantitative trait mapping. Genetics 138:963–971. https://doi.org/10.1093/genetics/138.3.963

Cucinotta M, Colombo L, Roig-Villanova I (2014) Ovule development, a new model for lateral organ formation. Front Plant Sci 5:1–12. https://doi.org/10.3389/fpls.2014.00117

Cucinotta M, Manrique S, Guazzotti A et al (2016) Cytokinin response factors integrate auxin and cytokinin pathways for female reproductive organ development. Dev 143:4419–4424. https://doi.org/10.1242/dev.143545

Cucinotta M, Manrique S, Cuesta C et al (2018) CUP-SHAPED COTYLEDON1 (CUC1) and CUC2 regulate cytokinin homeostasis to determine ovule number in Arabidopsis. J Exp Bot 69:5169–5176. https://doi.org/10.1093/jxb/ery281

Debernardi JM, Greenwood JR, Jean Finnegan E et al (2020) APETALA 2-like genes AP2L2 and Q specify lemma identity and axillary floral meristem development in wheat. Plant J 101:171–187. https://doi.org/10.1111/tpj.14528

Drews GN, Koltunow AM (2011) The Female Gametophyte. Arab B 9:e0155. https://doi.org/10.1199/tab.0155

Elliott RC, Betzner AS, Huttner E et al (1996) AINTEGUMENTA, an APETALA2-like gene of arabidopsis with pleiotropic roles in ovule development and floral organ growth. Plant Cell 8:155–168. https://doi.org/10.1105/tpc.8.2.155

Fan C, Cai G, Qin J et al (2010) Mapping of quantitative trait loci and development of allele-specific markers for seed weight in Brassica napus. Theor Appl Genet 121:1289–1301. https://doi.org/10.1007/s00122-010-1388-4

Favaro R, Pinyopich A, Battaglia R et al (2003) MADS-box protein complexes control carpel and ovule development in Arabidopsis. Plant Cell 15:2603–2611. https://doi.org/10.1105/tpc.015123

Fourquin C, Primo A, Martínez-Fernández I et al (2014) The CRC orthologue from Pisum sativum shows conserved functions in carpel morphogenesis and vascular development. Ann Bot 114:1535–1544. https://doi.org/10.1093/aob/mcu129

Galbiati F, Sinha Roy D, Simonini S et al (2013) An integrative model of the control of ovule primordia formation. Plant J 76:446–455. https://doi.org/10.1111/tpj.12309

Hall MC, Basten CJ, Willis JH (2006) Pleiotropic quantitative trait loci contribute to population divergence in traits associated with life-history variation in Mimulus guttatus. Genetics 172:1829–1844. https://doi.org/10.1534/genetics.105.051227

He Y, Wu D, Wei D et al (2017) GWAS, QTL mapping and gene expression analyses in Brassica napus reveal genetic control of branching morphogenesis. Sci Rep 7:1–9. https://doi.org/10.1038/s41598-017-15976-4

He X, Liu W, Li W et al (2020) Genome-wide identification and expression analysis of CaM/CML genes in Brassica napus under abiotic stress. J Plant Physiol 255:153251. https://doi.org/10.1016/j.jplph.2020.153251

Hu GL, Zhang DL, Pan HQ et al (2011) Fine mapping of the awn gene on chromosome 4 in rice by association and linkage analyses. Chinese Sci Bull 56:835–839. https://doi.org/10.1007/s11434-010-4181-5

Huang HY, Jiang WB, Hu YW et al (2013) BR signal influences arabidopsis ovule and seed number through regulating related genes expression by BZR1. Mol Plant 6:456–469. https://doi.org/10.1093/mp/sss070

Ikram M, Han X, Zuo J-F et al (2020) Identification of QTNs and their candidate genes for 100-seed weight in soybean (Glycine max L) using multi-locus genome-wide association studies. Genes (Basel) 11:714. https://doi.org/10.3390/genes11070714

Ishida T, Aida M, Takada S, Tasaka M (2000) Involvement of CUP-SHAPED COTYLEDON genes in gynoecium and ovule development in Arabidopsis thaliana. Plant Cell Physiol 41:60–67. https://doi.org/10.1093/pcp/41.1.60

Jiang Z, Xu G, Jing Y et al (2016) Phytochrome B and REVEILLE1/2-mediated signalling controls seed dormancy and germination in Arabidopsis. Nat Commun 7:12377. https://doi.org/10.1038/ncomms12377

Jiao Y, Zhang K, Cai G et al (2021) Fine mapping and candidate gene analysis of a major locus controlling ovule abortion and seed number per silique in Brassica napus L. Theor Appl Genet 134:2517–2530. https://doi.org/10.1007/s00122-021-03839-6

Kelley DR, Gasser CS (2009) Ovule development: genetic trends and evolutionary considerations. Sex Plant Reprod 22:229–234. https://doi.org/10.1007/s00497-009-0107-2

Khan MN, Khan Z, Luo T et al (2020) Seed priming with gibberellic acid and melatonin in rapeseed: consequences for improving yield and seed quality under drought and non-stress conditions. Ind Crops Prod 156:112850. https://doi.org/10.1016/j.indcrop.2020.112850

Khan SU, Yangmiao J, Liu S, Zhang K, Khan MHU, Zhang Y, Olalekan A, Fan C, Zhou Y (2019) Genome-wide association studies in the genetic dissection of ovule number, seed number, and seed weight in Brassica napus L. Ind Crops Prod 142:111877. https://doi.org/10.1016/j.indcrop.2019.111877

Krizek BA (2009) AINTEGUMENTA and AINTEGUMENTA-LIKE6 act redundantly to regulate arabidopsis floral growth and patterning. Plant Physiol 150:1916–1929. https://doi.org/10.1104/pp.109.141119

Krolikowski KA, Victor JL, Wagler TN et al (2003) Isolation and characterization of the Arabidopsis organ fusion gene HOTHEAD. Plant J 35:501–511. https://doi.org/10.1046/j.1365-313X.2003.01824.x

Kuusk S, Sohlberg JJ, Long JA et al (2002) STY1 and STY2 promote the formation of apical tissues during Arabidopsis gynoecium development. Development 129:4707–4717. https://doi.org/10.1242/dev.129.20.4707

Li MX, Yeung JMY, Cherny SS, Sham PC (2012) Evaluating the effective numbers of independent tests and significant p-value thresholds in commercial genotyping arrays and public imputation reference datasets. Hum Genet 131:747–756. https://doi.org/10.1007/s00439-011-1118-2

Li F, Chen B, Xu K et al (2014) Genome-wide association study dissects the genetic architecture of seed weight and seed quality in rapeseed (Brassica napus L.). DNA Res 21:355–367. https://doi.org/10.1093/dnares/dsu002

Li S, Chen L, Zhang L et al (2015) BnaC9.SMG7b functions as a positive regulator of number of seeds per silique in rapeseed Brassica napus L by regulating the formation of functional female gametophytes. Plant Physiol 169:01040.2015. https://doi.org/10.1104/pp.15.01040

Li B, Zhao W, Li D et al (2018) Genetic dissection of the mechanism of flowering time based on an environmentally stable and specific QTL in Brassica napus. Plant Sci 277:296–310. https://doi.org/10.1016/j.plantsci.2018.10.005

Li K, Zhou X, Sun X et al (2021) Coordination between MIDASIN 1-mediated ribosome biogenesis and auxin modulates plant development. J Exp Bot 72:2501–2513. https://doi.org/10.1093/jxb/erab025

Liao S, Wang L, Li J, Ruan Y (2020) Cell wall invertase is essential for ovule development through sugar signaling rather than provision of carbon nutrients. Plant Physiol 183:1126–1144. https://doi.org/10.1104/pp.20.00400

Liu Z, Franks RG, Klink VP (2000) Regulation of gynoecium marginal tissue formation by LEUNIG and AINTEGUMENTA. Plant Cell 12:1879–1891. https://doi.org/10.1105/tpc.12.10.1879

Liu R, Gong J, Xiao X et al (2018) GWAS analysis and QTL identification of fiber quality traits and yield components in upland cotton using enriched high-density snp markers. Front Plant Sci 9:1–15. https://doi.org/10.3389/fpls.2018.01067

Liu H, Zou M, Zhang B et al (2022) Genome-wide association study identifies candidate genes and favorable haplotypes for seed yield in Brassica napus. Mol Breed 42:61. https://doi.org/10.1007/s11032-022-01332-6

Liu Y, Li X, Li K, Liu H, Lin C (2013) Multiple bHLH proteins form heterodimers to mediate CRY2-dependent regulation of flowering-time in Arabidopsis. PLoS Genet 9(10):e1003861. https://doi.org/10.1371/journal.pgen.1003861

Lolle SJ, Hsu W, Pruitt RE (1998) Genetic analysis of organ fusion in Arabidopsis thaliana. Genetics 149:607–619. https://doi.org/10.1093/genetics/149.2.607

Mantegazza O, Gregis V, Mendes MA et al (2014) Analysis of the arabidopsis REM gene family predicts functions during flower development. Ann Bot 114:1507–1515. https://doi.org/10.1093/aob/mcu124

McCouch SR, Cho Y, Yano M, Paul E, Blinstrub M, Morishima H et al (1997) Report on QTL nomenclature. Rice Genet Newlett 14:11–13

Modrusan Z, Reiser L, Feldmann KA et al (1994) Homeotic transformation of ovules into carpel-like structures in arabidopsis. Plant Cell 6:333–349. https://doi.org/10.2307/3869754

Nahar MAU, Ishida T, Smyth DR et al (2012) Interactions of CUP-SHAPED COTYLEDON and SPATULA genes control carpel margin development in Arabidopsis thaliana. Plant Cell Physiol 53:1134–1143. https://doi.org/10.1093/pcp/pcs057

Ni W, Xie D, Hobbie L et al (2004) Regulation of flower development in Arabidopsis by *SCF* complexes. Plant Physiol 134:1574–1585. https://doi.org/10.1104/pp.103.031971

Nie S, Zhang M, Zhang L (2017) Genome-wide identification and expression analysis of calmodulin-like (CML) genes in Chinese cabbage (Brassica rapa L. ssp. pekinensis). BMC Genomics 18:1–12. https://doi.org/10.1186/s12864-017-4240-2

Nole-Wilson S, Azhakanandam S, Franks RG (2010) Polar auxin transport together with AINTEGUMENTA and REVOLUTA coordinate early Arabidopsis gynoecium development. Dev Biol 346:181–195. https://doi.org/10.1016/j.ydbio.2010.07.016

Nordborg M, Weigel D (2008) Next-generation genetics in plants. Nature 456:720–723. https://doi.org/10.1038/nature07629

Orashakova S, Lange M, Lange S et al (2009) The CRABS CLAW ortholog from California poppy (Eschscholzia californica, Papaveraceae), EcCRC, is involved in floral meristem termination, gynoecium differentiation and ovule initiation. Plant J 58:682–693. https://doi.org/10.1111/j.1365-313X.2009.03807.x

Pagnussat GC, Yu HJ, Ngo QA et al (2005) Genetic and molecular identification of genes required for female gametophyte development and function in Arabidopsis. Development 132:603–614. https://doi.org/10.1242/dev.01595

Petrella R, Caselli F, Roig-Villanova I et al (2020) BPC transcription factors and a Polycomb Group protein confine the expression of the ovule identity gene SEEDSTICK in Arabidopsis. Plant J 102:582–599. https://doi.org/10.1111/tpj.14673

Pinyopich A, Ditta GS, Savidge B et al (2003) Assessing the redundancy of MADS-box genes during carpel and ovule development. Nature 424:85–88. https://doi.org/10.1038/nature01741

Qadir M, Wang X, Shah SRU et al (2021) Molecular network for regulation of ovule number in plants. Int J Mol Sci 22:12965. https://doi.org/10.3390/ijms222312965

Qadir M, Qin L, Ye J et al (2022) Genetic dissection of the natural variation of ovule number per ovary in oilseed rape germplasm (Brassica napus L.). Front Plant Sci 13:1–16. https://doi.org/10.3389/fpls.2022.999790

Raboanatahiry N, Chao H, Dalin H et al (2018) QTL alignment for seed yield and yield related traits in Brassica napus. Front Plant Sci 9:1–14. https://doi.org/10.3389/fpls.2018.01127

Raboanatahiry N, Chao H, He J, Li H, Yin Y, Li M (2022) Construction of a quantitative genomic map, identification and expression analysis of candidate genes for agronomic and disease-related traits in Brassica napus. Front Plant Sci 13:862363. https://doi.org/10.3389/fpls.2022.862363

Rawat R, Schwartz J, Jones MA et al (2009) REVEILLE1, a Myb-like transcription factor, integrates the circadian clock and auxin pathways. Proc Natl Acad Sci U S A 106:16883–16888. https://doi.org/10.1073/pnas.0813035106

Saha P, Ray T, Tang Y et al (2013) Self-rescue of an EXTENSIN mutant reveals alternative gene expression programs and candidate proteins for new cell wall assembly in Arabidopsis. Plant J 75:104–116. https://doi.org/10.1111/tpj.12204

Shi D, Yang W (2011) Ovule development in Arabidopsis : progress and challenge. Curr Opin Plant Biol 14:74–80. https://doi.org/10.1016/j.pbi.2010.09.001

Shi J, Li R, Qiu D et al (2009) Unraveling the complex trait of crop yield with quantitative trait loci mapping in *Brassica napus*. Genetics 182:851–861. https://doi.org/10.1534/genetics.109.101642

Shi J, Li R, Zou J et al (2011) A dynamic and complex network regulates the heterosis of yield-correlated traits in rapeseed Brassica napus L. PLoS One 6(7):e21645. https://doi.org/10.1371/journal.pone.0021645

Shi J, Zhan J, Yang Y et al (2015) Linkage and regional association analysis reveal two new tightly-linked major-QTLs for pod number and seed number per pod in rapeseed (Brassica napus L.). Sci Rep 5:1–18. https://doi.org/10.1038/srep14481

Skinner DJ (2004) Regulation of ovule development. PLANT CELL ONLINE 16:S32–S45. https://doi.org/10.1105/tpc.015933

Skinner DJ, Baker SC, Meister RJ et al (2001) The Arabidopsis HUELLENLOS gene, which is essential for normal ovule development, encodes a mitochondrial ribosomal protein. Plant Cell 13:2719–2730. https://doi.org/10.1105/tpc.13.12.2719

Skinner DJ, Gasser CS (2009) Expression-based discovery of candidate ovule development regulators through transcriptional profiling of ovule mutants. BMC Plant Biol 9:29. https://doi.org/10.1186/1471-2229-9-29

Tang S, Zhao H, Lu S et al (2021) Genome- and transcriptome-wide association studies provide insights into the genetic basis of natural variation of seed oil content in Brassica napus. Mol Plant 14:470–487. https://doi.org/10.1016/j.molp.2020.12.003

Tsai YC, Delk NA, Chowdhury NI, Braam J (2007) Arabidopsis potential calcium sensors regulate nitric oxide levels and the transition to flowering. Plant Signal Behav 2:446–454. https://doi.org/10.4161/psb.2.6.4695

Wang G, Schmalenbach I, von Korff M et al (2010) Association of barley photoperiod and vernalization genes with QTLs for flowering time and agronomic traits in a BC2DH population and a set of wild barley introgression lines. Theor Appl Genet 120:1559–1574. https://doi.org/10.1007/s00122-010-1276-y

Wang X, Chen L, Wang A et al (2016) Quantitative trait loci analysis and genome-wide comparison for silique related traits in Brassica napus. BMC Plant Biol 16:1–15. https://doi.org/10.1186/s12870-016-0759-7

Wang H, Yan M, Xiong M et al (2020) Genetic dissection of thousand - seed weight and fine mapping of cqSW. A03–2 via linkage and association analysis in rapeseed (Brassica napus L.). Theor Appl Genet 133:1321–1335. https://doi.org/10.1007/s00122-020-03553-9

Wang T, Wei L, Wang J et al (2020b) Biotechnology for biofuels integrating GWAS, linkage mapping and gene

expression analyses reveals the genetic control of growth period traits in rapeseed (Brassica napus L.). Biotechnol Biofuels 13:134. https://doi.org/10.1186/s13068-020-01774-0

Xin S, Dong H, Yang L et al (2021) Both overlapping and independent loci underlie seed number per pod and seed weight in Brassica napus by comparative quantitative trait loci analysis. Mol Breed 41:41. https://doi.org/10.1007/s11032-021-01232-1

Yang Y, Wang Y, Zhan J et al (2017) Genetic and cytological analyses of the natural variation of seed number per pod in rapeseed (Brassica napus L.). Front Plant Sci 8:1–14. https://doi.org/10.3389/fpls.2017.01890

Yuan J, Kessler SA (2019) A genome-wide association study reveals a novel regulator of ovule number and fertility in Arabidopsis thaliana. PLoS Genet 15:1–25. https://doi.org/10.1371/journal.pgen.1007934

Zhang J, Wrage EL, Vankova R et al (2006) Over-expression of *SOB5* suggests the involvement of a novel plant protein in cytokinin-mediated development. Plant J 46:834–848. https://doi.org/10.1111/j.1365-313X.2006.02745.x

Zhang J, Vankova R, Malbeck J et al (2009) AtSOFL1 and atSOFL2 act redundantly as positive modulators of the endogenous content of specific cytokinins in Arabidopsis. PLoS ONE 4:1–11. https://doi.org/10.1371/journal.pone.0008236

Zhao W, Wang X, Wang H et al (2016) Genome-wide identification of QTL for seed yield and yield-related traits and construction of a high-density consensus Map for QTL Comparison in *Brassica napus*. Front Plant Sci 7:1–14. https://doi.org/10.3389/fpls.2016.00017

Zhao W, Zhang L, Chao H et al (2019) Genome-wide identification of silique-related traits based on high-density genetic linkage map in Brassica napus. Mol Breed 39:86. https://doi.org/10.1007/s11032-019-0988-1

Zhao-Baang Z (1994) Precision mapping of quantitative trait loci. Genetics 36(4):1457–68. https://doi.org/10.1093/genetics/136.4.1457

Zhu Y, Ye J, Zhan J et al (2020) Validation and characterization of a seed number per silique quantitative trait locus qSN.A7 in rapeseed (Brassica napus L.). Front Plant Sci 11:1–11. https://doi.org/10.3389/fpls.2020.00068

Publisher's Note Springer Nature remains neutral with regard to jurisdictional claims in published maps and institutional affiliations.

Springer Nature or its licensor (e.g. a society or other partner) holds exclusive rights to this article under a publishing agreement with the author(s) or other rightsholder(s); author self-archiving of the accepted manuscript version of this article is solely governed by the terms of such publishing agreement and applicable law.